

Supporting Information

Coassembly-Induced Transformation of Dipeptide Amyloid-Like Structures into Stimuli-Responsive Supramolecular Materials

Wei Ji,[†] Chengqian Yuan,[‡] Priyadarshi Chakraborty,[†] Pandeewar Makam,[†] Santu Bera,[†] Sigal Rencus-Lazar,[†] Junbai Li,^{§,*} Xuehai Yan,^{‡,*} and Ehud Gazit^{†,#,*}

[†]School of Molecular Cell Biology and Biotechnology, George S. Wise Faculty of Life Sciences, Tel Aviv University, Tel Aviv 6997801, Israel.

[‡]State Key Laboratory of Biochemical Engineering, Institute of Process Engineering, Chinese Academy of Sciences, Beijing 100190, China.

[§]Beijing National Laboratory for Molecular Sciences, CAS Key Lab of Colloid Interface and Chemical Thermodynamics, Institute of Chemistry, Chinese Academy of Sciences, Beijing 100190, China.

[#]Department of Materials Science and Engineering, Iby and Aladar Fleischman Faculty of Engineering, Tel Aviv University, Tel Aviv 6997801, Israel.

*Email: ehudg@post.tau.ac.il; yanxh@ipe.ac.cn; jbli@iccas.ac.cn

Experimental Procedures

Materials: All solvents and chemicals are commercially available. Chemicals were used without further purification. Water was processed using a Millipore purification system (Darmstadt, Germany) with a minimum resistivity of 18.2 M Ω cm. FmocFF, BPE, and DPDS were purchased from Sigma at a purity level of >95%, and ultrapure water was obtained from Biological Industries. ¹H NMR spectra were recorded on a Bruker Advance 400 MHz spectrometer.

Rheology: Mechanical properties measurements were performed on an ARES-G2 rheometer (TA Instruments, New Castle, DE, USA) using a 20 mm parallel-plate geometry with a gap of 1000 μ m. All the gels were allowed to age overnight before the measurements. Dynamic frequency sweep experiments of the gels were carried out at a constant strain of 0.1% between 0.01-10 Hz. Strain sweep experiments of gels were carried out at a constant frequency of 1 Hz between 0.1%-200%.

¹H NMR test: The powders of individual FmocFF, FmocFF/BPE (1:1) and FmocFF/DPDS (1:1) were dissolved by heating to 50 °C in dimethyl sulfoxide-*d*₆ (DMSO-*d*₆) at a final FmocFF concentration of 4.0 mg/mL, keeping the same concentration with individual BPE and individual DPDS in the mixture of FmocFF/BPE (1:1) and FmocFF/DPDS (1:1). The ¹H NMR spectra were recorded on a Bruker Advance 400 MHz spectrometer.

Fluorescence spectrophotometry: The intensity of fluorescence emission of different gels was analysed using a FluoroMax-4 Spectrofluorometer (Horiba Jobin Yvon, Kyoto, Japan) at ambient temperature. The excitation wavelength was set at 450 nm and the emission wavelength was collected from 465 nm to 650 nm.

Fluorescence microscopy: Following ThT incubation, the gels were placed on a glass slide and observed using a Nikon Eclipse Ti-E fluorescence microscope at the GFP channel (Ex 450-490 nm, Em 500-550 nm).

UV-Vis spectra: UV-Vis spectra of the samples were recorded using a T60 UV-Vis spectrophotometer (PG instruments). A quartz cuvette with an optical path length of 1 mm was used.

Mass spectrometry (MS) spectra: MS was collected using an Acquity UPLC system coupled to a TQD XEVO triple quadrupole ESI source mass spectrometer system from Waters (Milford, MA,

USA). The positive electrospray ionization (ES⁺) channel was used for analysis.

Computational methods: All quantum chemical calculations were conducted on the Gaussian 09 package¹. Typical FmocFF/BPE dimers and trimers predominantly stabilized by the intermolecular hydrogen bonds were constructed and optimized at the level of B3LYP/6-31 g(d,p) theory. Harmonic vibrational frequency calculations on the optimized geometries were also performed to ensure the structures at local minima. The FmocFF/BPE binding energies (BE) were calculated as the energy difference between their molecular clusters and the sum of the energies of FmocFF and BPE (Eq. 1).

$$BE = E[(FmocFF)_m(BPE)_n] - mE(FmocFF) - nE(BPE). \quad (1)$$

AAMD simulations were performed using the Gromacs package (Version 5.1.4)². The general AMBER force field (GAFF) was used to model the Fmoc-FF and BPE molecules³. Water molecules were modelled using the tip3p potential. To derive the force field parameters within the framework of the GAFF, the geometry optimization and molecular electrostatic potential of Fmoc-FF and BPE were obtained at the level of HF/6-31 g(d) theory. The Antechamber package was then used to compute the partial charge according to the restrained electrostatic potential (RESP) formalism⁴. AAMD simulation was performed on water boxes containing the pre-constructed co-assemblies of 40 FmocFF and 40 BPE molecules. The solution was first minimized using the conjugate-gradient algorithm with a tolerance on the maximum force of 200 KJ/mol, and the temperature and volume of each system were equilibrated by running 400 ps of a constant volume, constant temperature (NVT) simulation, followed by 400 ps NPT simulations. Production runs in the NPT ensemble were then conducted for 20 ns. The leapfrog algorithm with a time step of 2 fs was used to integrate the equations of motion. The isothermal-isobaric (constant NPT) ensemble was used to maintain a temperature of 300 K and a pressure of 1 bar. The velocity rescale thermostat and the isotropic ParrinelloRahman barostat were used with relaxation times of 0.4 and 2.0 ps, respectively. The electrostatic forces were calculated by means of the particle-mesh Edwald approach with a cutoff of 1.0 nm. A 1.0 nm cutoff was also used for the van der Waals forces. The LINCS algorithm was applied at each step to preserve the bond lengths.

Cell viability: 3T3 mouse fibroblast cells were purchased from ATCC and cultured in Dulbecco's Modified Eagle's Medium (DMEM) supplemented with 10% fetal calf serum, 100 U mL⁻¹ penicillin, 100 U mL⁻¹ streptomycin, and 2 mmol L⁻¹ L-glutamine (all from Biological Industries,

Israel). The cells were cultured in a petri dish at 37 °C in a humidified atmosphere containing 5% CO₂. 100 μL FmocFF self-assembly, FmocFF/BPE, and FmocFF/DPDS co-assemblies at a series of concentrations (50-750 μM) were added into one well of 96 plate, respectively. The plate was dried by vacuum and 100 μL of cell suspension (2 x10⁵ cells/mL) was added to each well.⁵ Following incubation for 24 h at 37 °C, cell viability was evaluated using the 2,3-bis(2-methoxy-4-nitro-5-sulphophenyl)-2H-tetrazolium-5-carboxanilide (XTT) cell proliferation assay kit (Biological Industries, Israel) according to the manufacturer's instructions.⁶ Briefly, 100 μL of the activation reagent was added to 5 mL of the XTT reagent, followed by the addition of 50 μL of activated-XTT Solution to each well. After 2 h of incubation at 37 °C, color intensity was measured using an ELISA microplate reader at 450 nm and 630 nm. Results are presented as mean and the standard error of the mean. Each experiment was repeated for a minimum of three times.

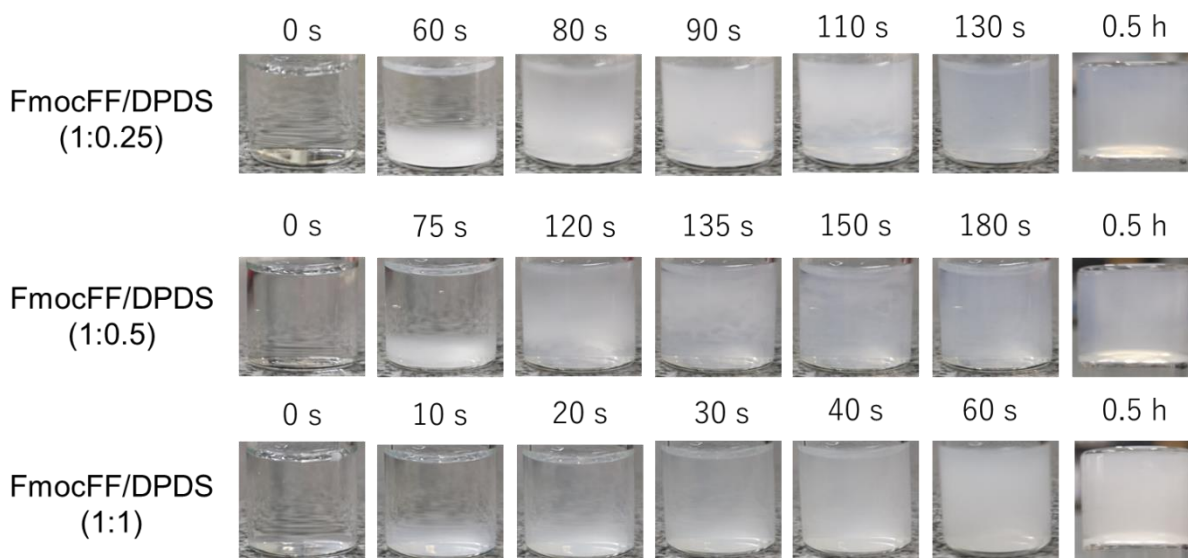


Figure S1. Time lapse optical images of FmocFF/DPDS (1:0.25), FmocFF/DPDS (1:0.5), and FmocFF/DPDS (1:1) at a concentration of 2 mg/mL.

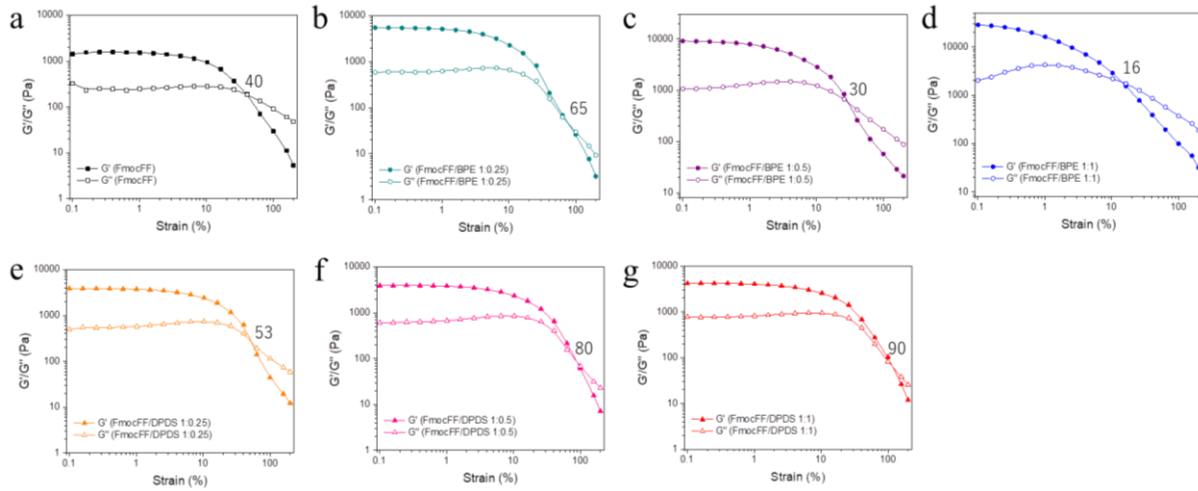


Figure S2. Rheological strain sweep measurements of different hydrogels at a constant frequency of 1 Hz. (a) FmocFF, (b) 1:0.25 FmocFF/BPE, (c) 1:0.5 FmocFF/BPE, (d) 1:1 FmocFF/BPE, (e) 1:0.25 FmocFF/DPDS, (f) 1:0.5 FmocFF/DPDS, and (g) 1:1 FmocFF/DPDS.

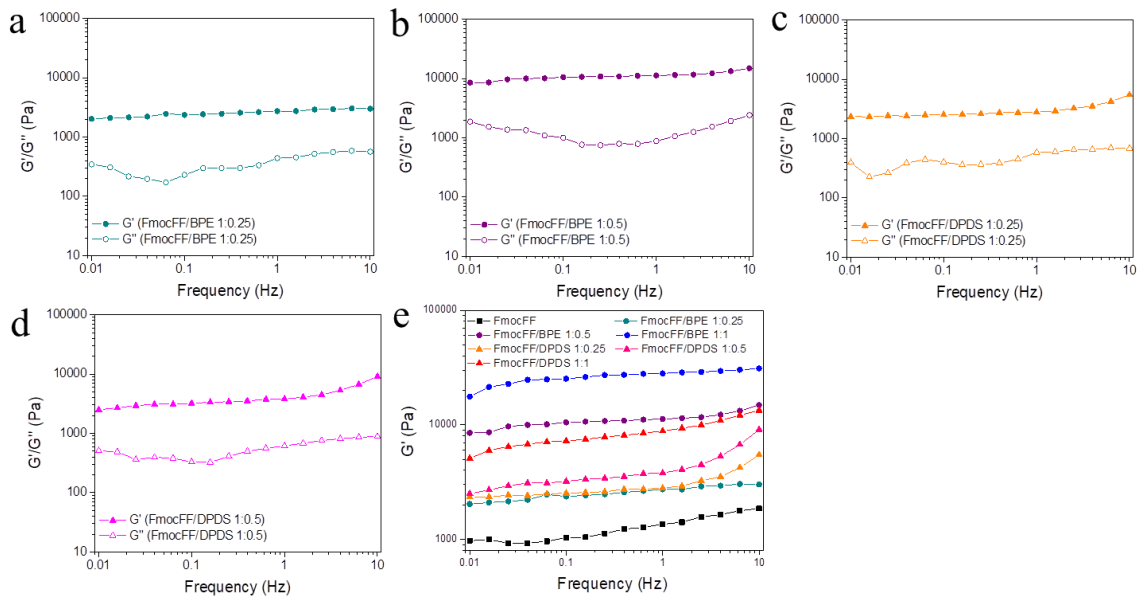


Figure S3. (a-d) Rheological dynamic frequency sweep measurements of different gels at a strain of 0.1% over a range of 0.01-10 rad s^{-1} . (a) 1:0.25 FmocFF/BPE, (b) 1:0.5 FmocFF/BPE, (c) 1:0.25 FmocFF/DPDS, (d) 1:0.5 FmocFF/DPDS. (e) Storage modulus (G') of the gels, as indicated.

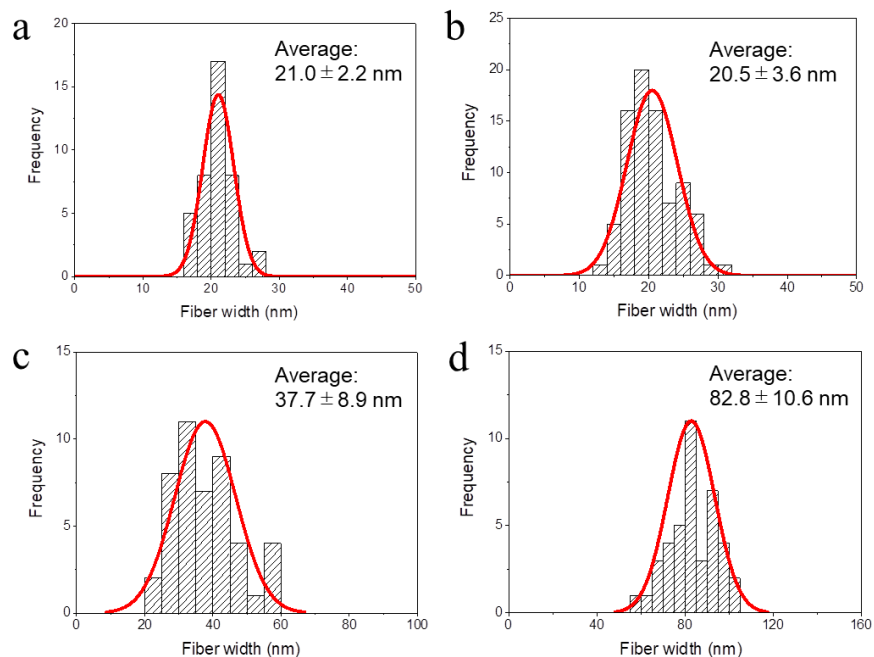


Figure S4. Average size distribution histogram of the nanofibrils in the gels. (a) FmocFF, (b) 1:0.25 FmocFF/BPE, (c) 1:0.5 FmocFF/BPE, and (d) 1:1 FmocFF/BPE

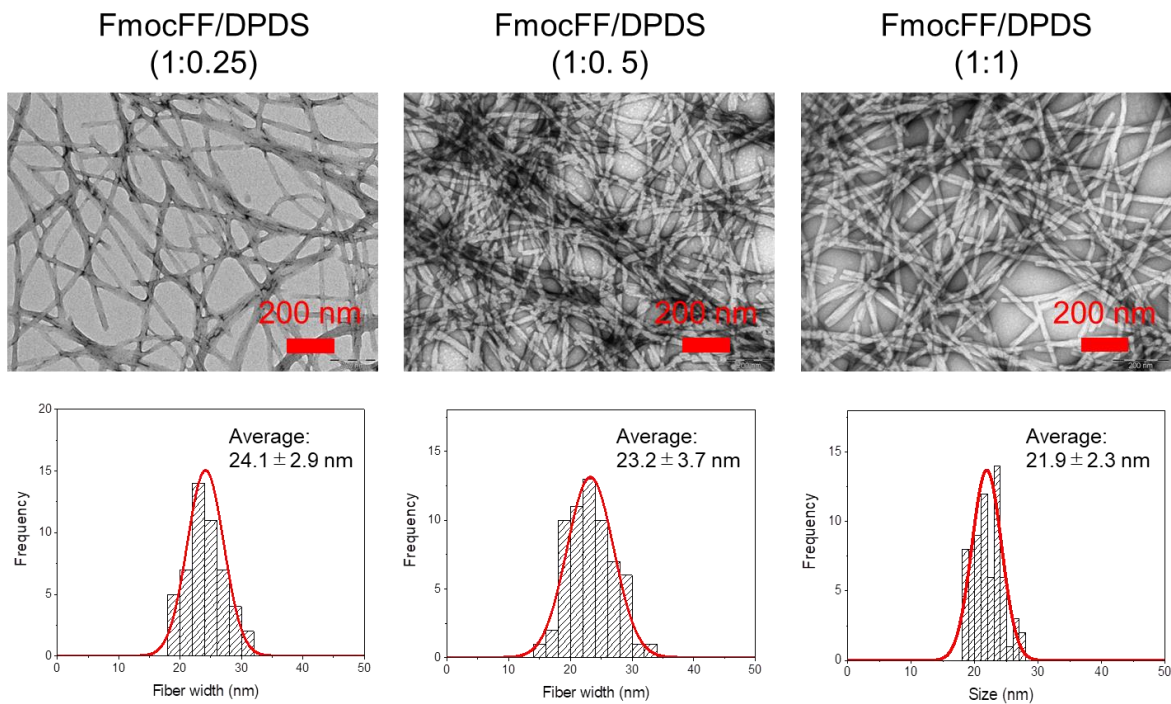


Figure S5. TEM images (top) and average size distribution histograms (bottom) of FmocFF/DPDS at ratios of 1:0.25, 1:0.5, 1:1, as indicated. Scale bar is 200 nm.

Table S1. Peak assignments of powder XRD patterns.

BPE		FmocFF/BPE		DPDS		FmocFF/DPDS	
2 θ (°)	d (Å)						
14.01	6.3	7.15	12.4	17.66	5	6.96	12.7
16.66	5.3	10.88	8.1	18.72	4.7	14.35	6.2
17.54	5.1	13.54	6.5	20.28	4.4	15.05	5.9
20.46	4.3	14.42	6.1	21.22	4.2	18.19	4.9
21.28	4.2	17.2	5.2	21.97	4	18.77	4.7
21.95	4	20.05	4.4	23.02	3.9	19.64	4.5
22.63	3.9	21.14	4.2	24.42	3.6	20.23	4.4
24.2	3.7			26.63	3.3	21.68	4.1
26.84	3.3			27.74	3.2	23.08	3.9
28.2	3.2			30.64	2.9	23.84	3.7
33.84	2.6					24.42	3.6

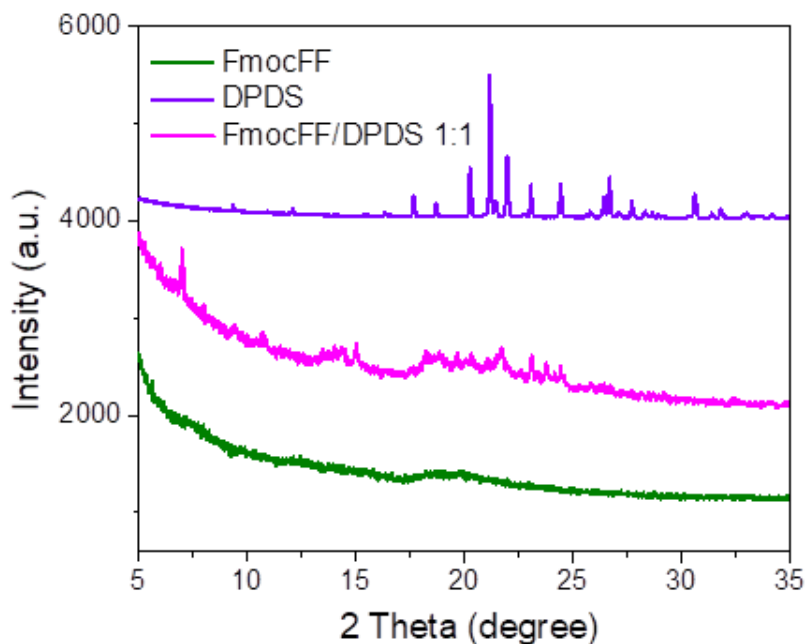


Figure S6. Powder XRD patterns of FmocFF gel (green), DPDS powder (blue), and FmocFF/DPDS (1:1) gel (pink).

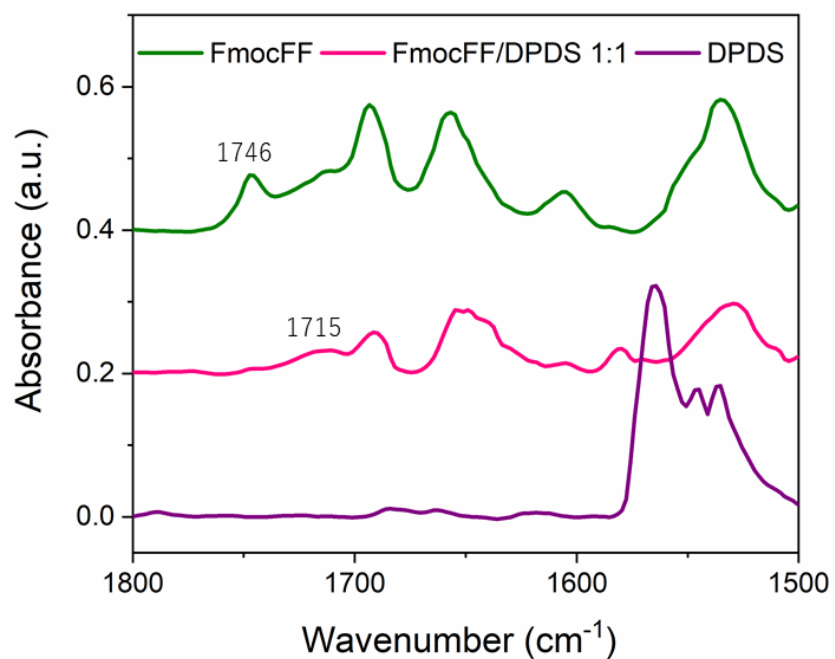


Figure S7. FTIR spectra of FmocFF gel (green), DPDS powder (purple), and FmocFF/DPDS (1:1) gel (pink).

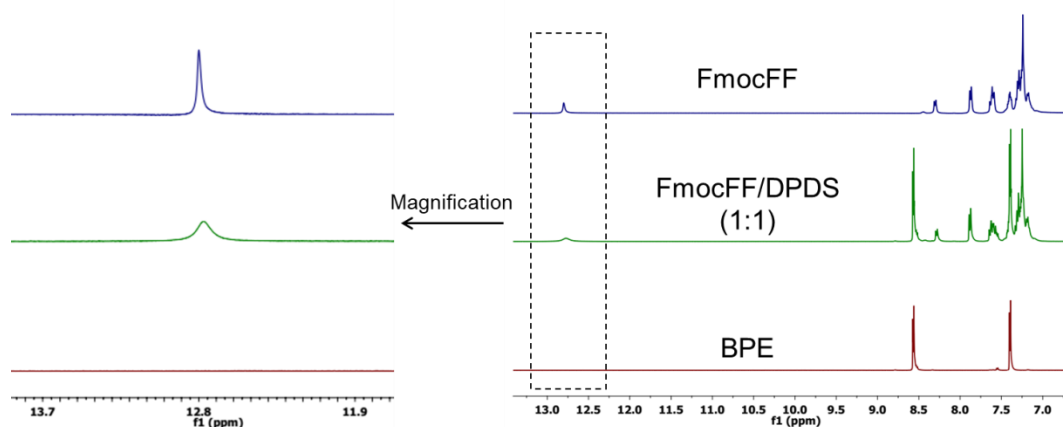


Figure S8. Right: ^1H NMR spectra of FmocFF, DPDS, and the FmocFF/DPDS mixture in $\text{DMSO-}d_6$. Left: magnification of the area marked in the spectra on the right corresponding to the proton signal of COOH.

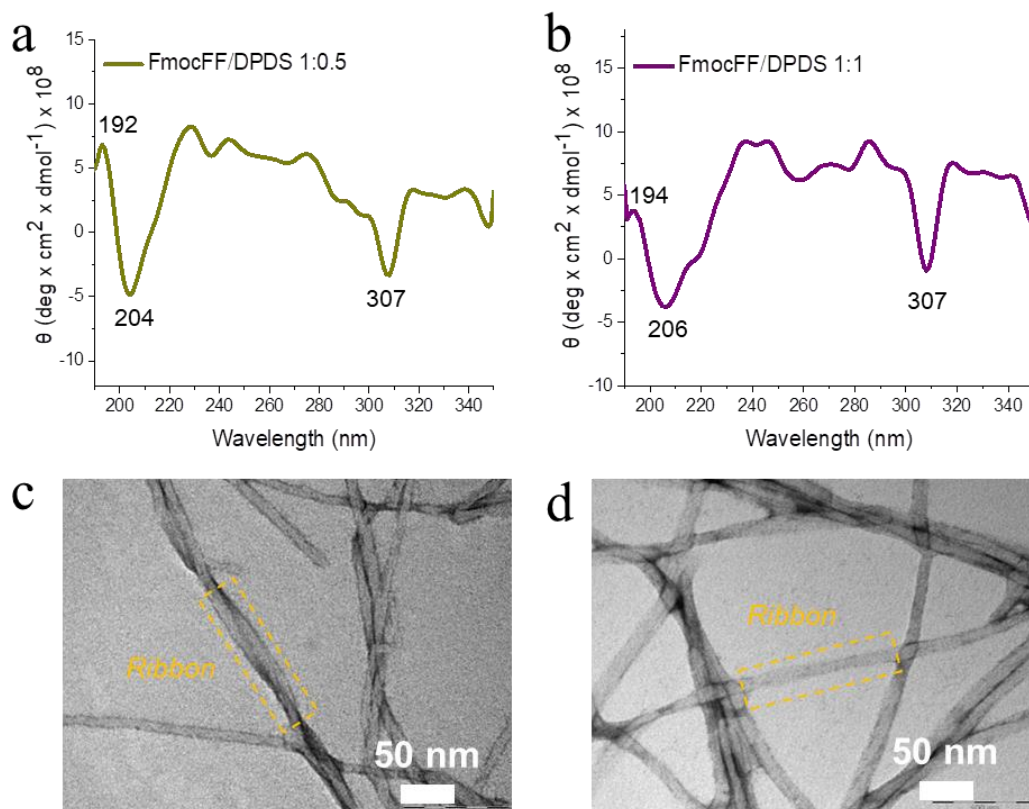


Figure S9. (a, b) CD spectra and (c, d) high-resolution TEM images of co-assembled FmocFF/DPDS gels at a concentration of 2 mg/mL. (a, c) 1:0.5 FmocFF/DPDS FmocFF, (b, d) 1:1 FmocFF/DPDS FmocFF.

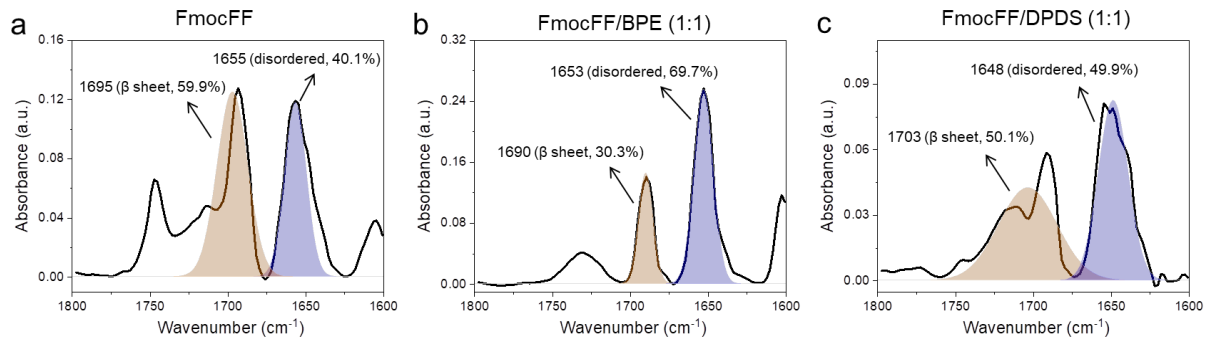


Figure S10. FTIR analysis of the secondary structures of FmocFF, FmocFF/BPE (1:1) and FmocFF/DPDS (1:1) fitted by multiple Gaussian peaks.

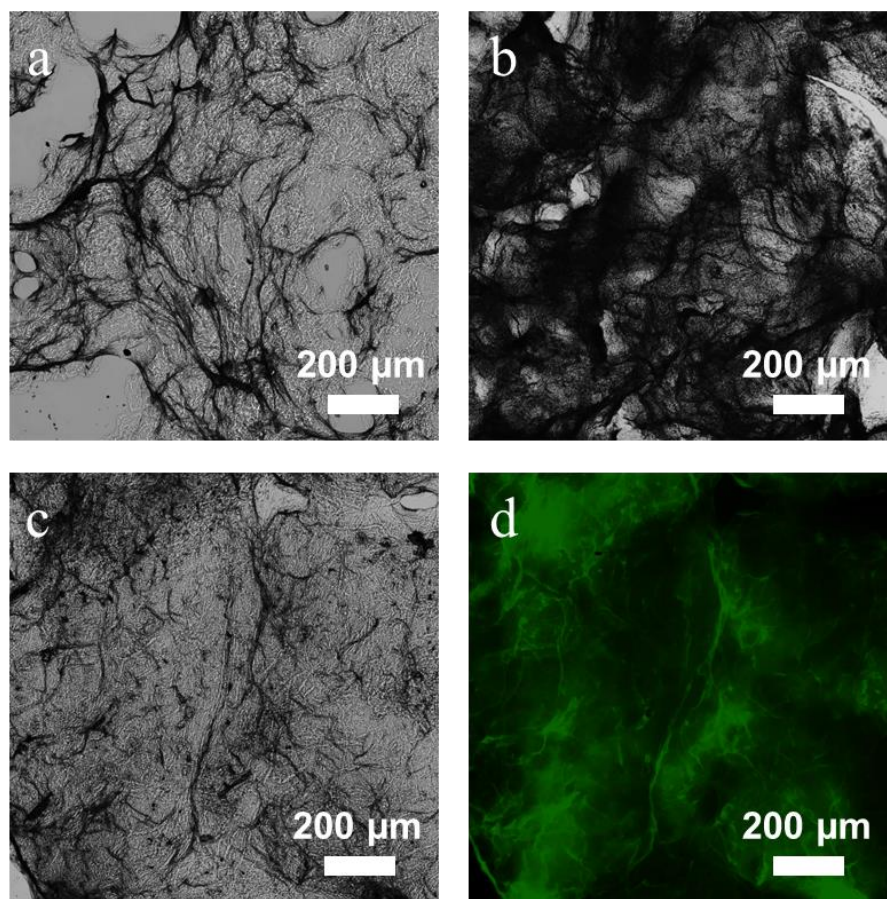


Figure S11. (a-c) Bright field images of (a) FmocFF, (b) FmocFF/BPE, and (c) FmocFF/DPDS. (d) Fluorescence microscopy image of FmocFF/DPDS (1:1) incubated with ThT. Scale bar is 200 μm .

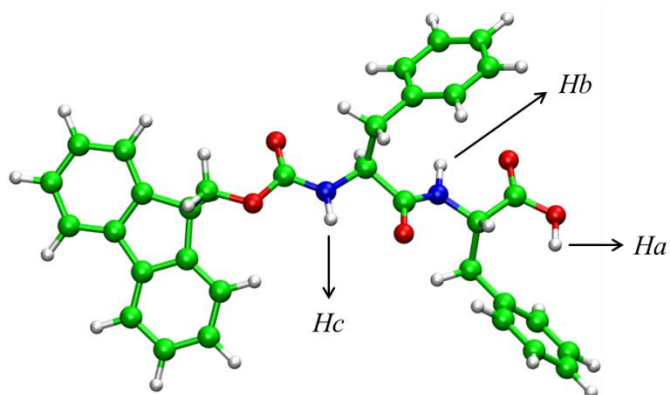


Figure S12. Three types of hydrogen atoms (Ha, Hb, Hc) in FmocFF can potentially form hydrogen bonds with the nitrogen atom in the pyridine ring of BPE.

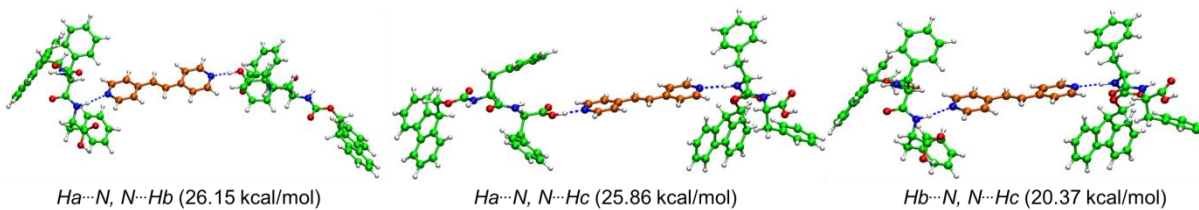


Figure S13. Multiple trimers of FmocFF and BPE connected by different hydrogen bonding interaction modes in the 2:1 FmocFF/BPE mixture. The corresponding binding energy is shown below the molecular packing patterns.

Table S2. Bond length of the hydrogen bonds and the binding energy of FmocFF and BPE dimers and trimers with multiple hydrogen bonding interaction modes. The shortest bond length and highest binding energy suggest the most stable hydrogen bond interaction mode for dimers of 1:1 FmocFF/BPE or trimers of 2:1 FmocFF/BPE.

	Hydrogen bonds	Bond length (Å)	Binding energy (kcal/mol)
Dimers of 1:1 FmocFF/BPE	Ha···N	1.68	15.87
	Hb···N	2.01	10.31
	Hc···N	2.03	10.02
Trimers of 2:1 FmocFF/BPE	Ha···N, N···Ha	1.69, 1.69	31.14
	Hb···N, N···Hb	2.03, 2.03	20.45
	Hc···N, N···Hc	2.02, 2.04	20.02
	Ha···N, N···Hb	1.68, 2.03	26.15
	Ha···N, N···Hc	1.68, 2.03	25.86
	Hb···N, N···Hc	2.03, 2.03	20.37

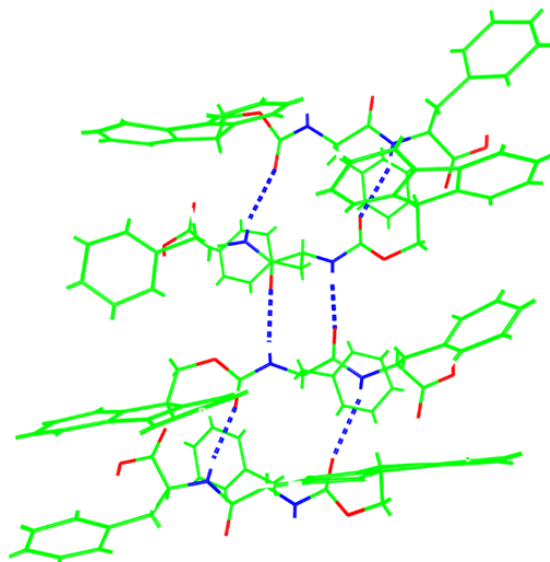


Figure S14. The building block of individual FmocFF clusters with β -sheet hydrogen bonding. The dashed blue lines denote the intermolecular hydrogen bonds between FmocFF molecules.

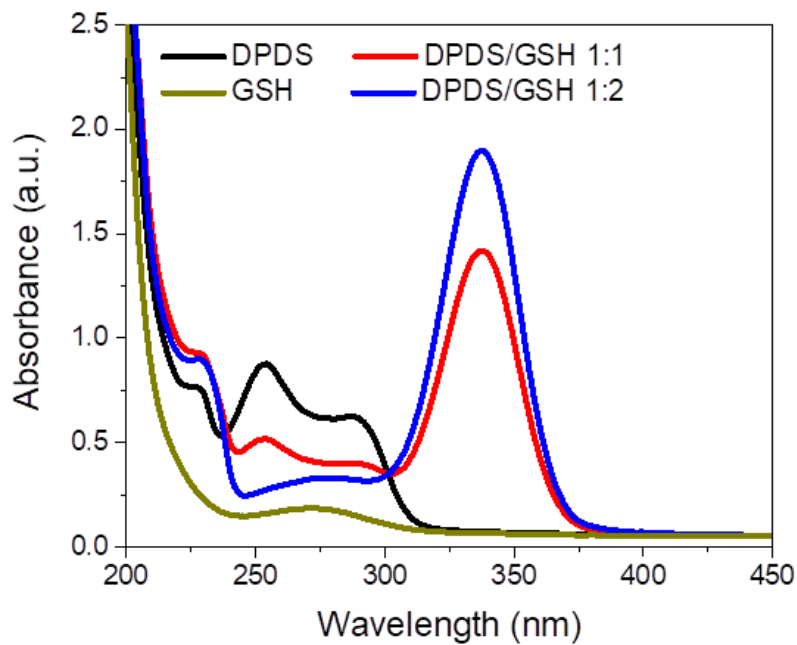


Figure S15. Absorption spectrum of DPDS (black), GSH (dark green), 1:1 DPDS/GSH (red), and 1:2 FmocFF/GSH (blue). The molar concentration of DPDS is 100 μ M in the single- and two-component samples.

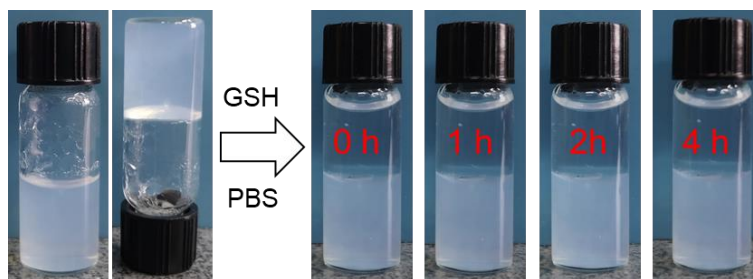


Figure S16. No responsiveness of individual FmocFF in the presence of GSH (100 mM) in PBS.

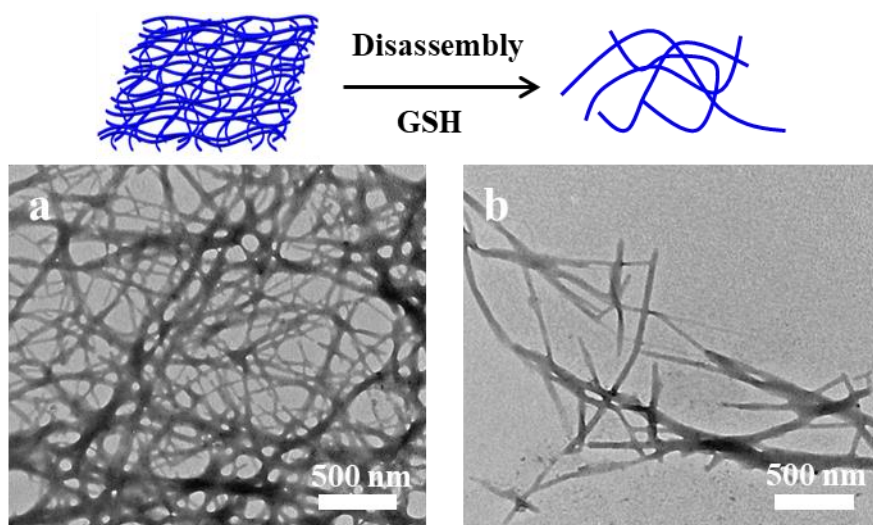


Figure S17. TEM images of the FmocFF/DPDS gel in the presence of GSH (100 mM) at (a) 0 h and (b) 4 h. Scale bar is 500 nm.

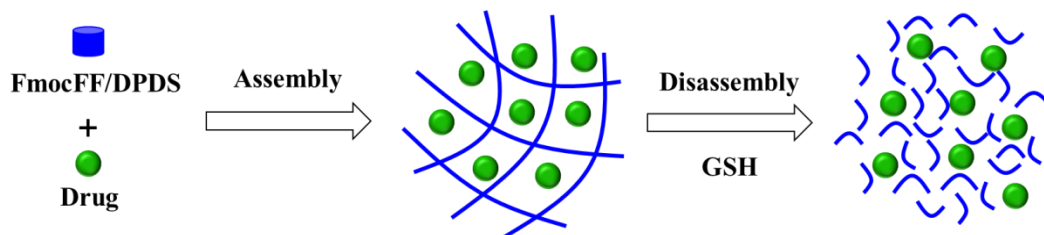


Figure S18. Schematic presentation of drug loading in the FmocFF/DPDS co-assembled networks and controllable release in the presence of the GSH reducing agent.

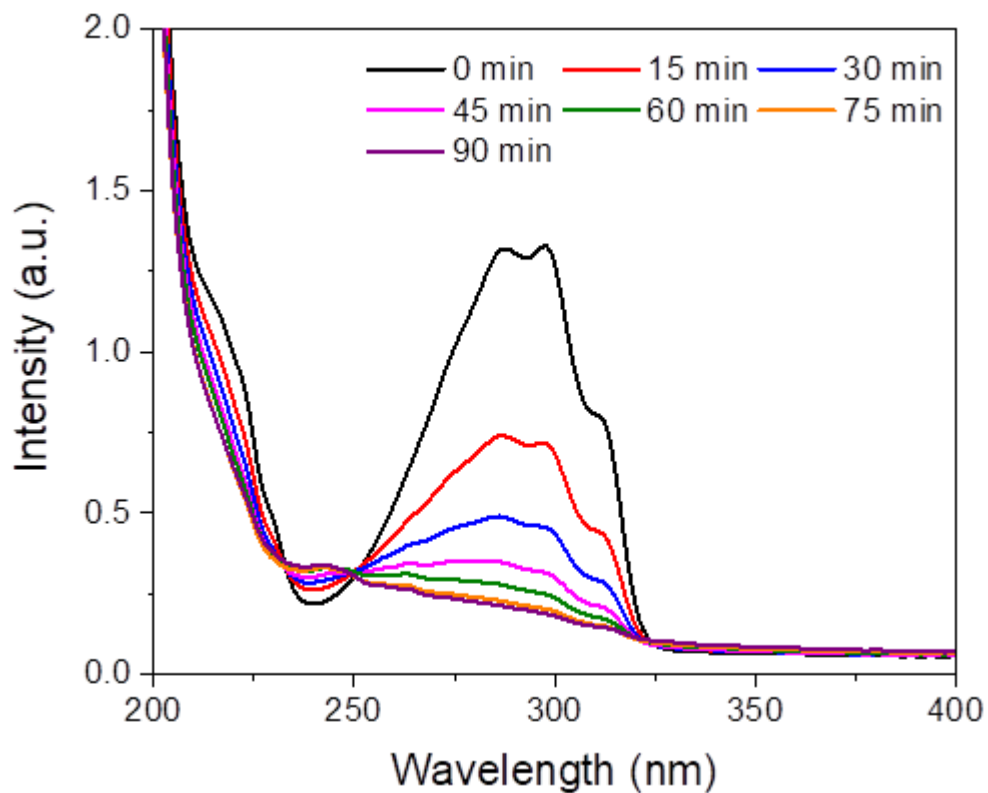


Figure S19. UV-Vis absorption traces of BPE (50 μM) in water by UV irradiation with irradiation times varying from 0 to 90 min. Samples were analysed after the specified irradiation time by a handheld UV lamp (6 watts) at 365 nm.



Figure S20. No photo-induced emission for individual FmocFF hydrogel under UV light irradiation.

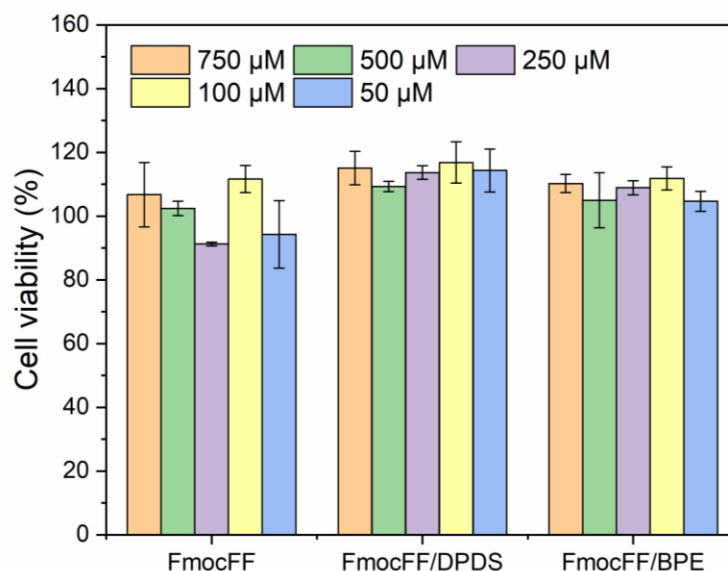


Figure S21. XTT viability assays of 3T3 mouse fibroblast cells incubated for 24 h with different concentrations of FmocFF assemblies.

References

1. Frisch, M. J.; Trucks, G. W.; Schlegel, H. B. *Gaussian 09*, revision D.01; Gaussian, Inc.: Wallingford, CT, **2013**.
2. Abraham, M. J.; Murtola, T.; Schulz, R.; Páll, S.; Smith, J. C.; Hess, B.; Lindahl, E. GROMACS: High Performance Molecular Simulations through Multi-Level Parallelism from Laptops to Supercomputers. *SoftwareX* **2015**, *1*, 19-25.
3. Wang, J., Wolf, R.M., Caldwell, J.W., Kollman, P.A., Case, D.A. Development and Testing of a General Amber Force Field. *J. Comput. Chem.* **2004**, *25*, 1157-1174.
4. Wang, J.; Wang, W.; Kollman, P.; Case, D. Antechamber: An Accessory Software Package for Molecular Mechanical Calculations. *J. Am. Chem. Soc.* **2001**, *222*, 403-444.
5. Dou, X. Q., Li, P., Zhang, D., Feng, C. L. RGD Anchored C2-Benzene Based PEG-Like Hydrogels as Scaffolds for Two and Three Dimensional Cell Cultures. *J. Mater. Chem. B* **2013**, *1*, 3562-3568.
6. Paul, A., Viswanathan, G. K., Mahapatra, S., Balboni, G., Pacifico, S., Gazit, E., Segal, D. Antagonistic Activity of Naphthoquinone-Based Hybrids toward Amyloids Associated with Alzheimer's Disease and Type-2 Diabetes. *ACS Chem. Neurosci.* **2019**, *10*, 3510-3520.